CHAPTER IV

OPTICAL AND MAGNETIC STUDIES OF DIVALENT $3d^8$ ION IN $CsCdCl_3$ AT LOW TEMPERATURE

Since the valency state of vanadium in its doped crystal prepared by us could not be properly estimated, we measured the absorption spectrum and magnetic susceptibility and anisotropy of the nickel doped crystal, $CsCdCl_3 : Ni^{2+}$ only.

RESULTS AND DISCUSSION

I. Optical Studies

The configuration of eight 3d electrons permits the states ^3F, ^3P, ^1D, ^1G and ^1S states, of which according to Hund's rule ^3F lies lowest. Of the three stark levels in which the ground ^3F splits under an octahedral environment, the non-degenerate $^3A_{2g}$ lies lowest. The other two are triply degenerate, $^3T_{2g}$ and $^3T_{1g}$ in order of increasing energy. The separation of this level from the lowest orbital non-degenerate $^3A_{2g}$ state is 10 Dq and 18 Dq, respectively (Fig. 16).

In order to explain our room temperature spectrum (Fig. 17a dotted line) we have ignored the effect of spin-orbit interaction in the first trial calculation. Of the three spin allowed transitions, the broad band (Fig. 17a) from 5650 cm^{-1} to 6000 cm^{-1} has been ascribed to $^3A_{2g} \longrightarrow {}^3T_{2g}$ transition. Taking the centre of the band at 5850 cm^{-1}, the value of Dq

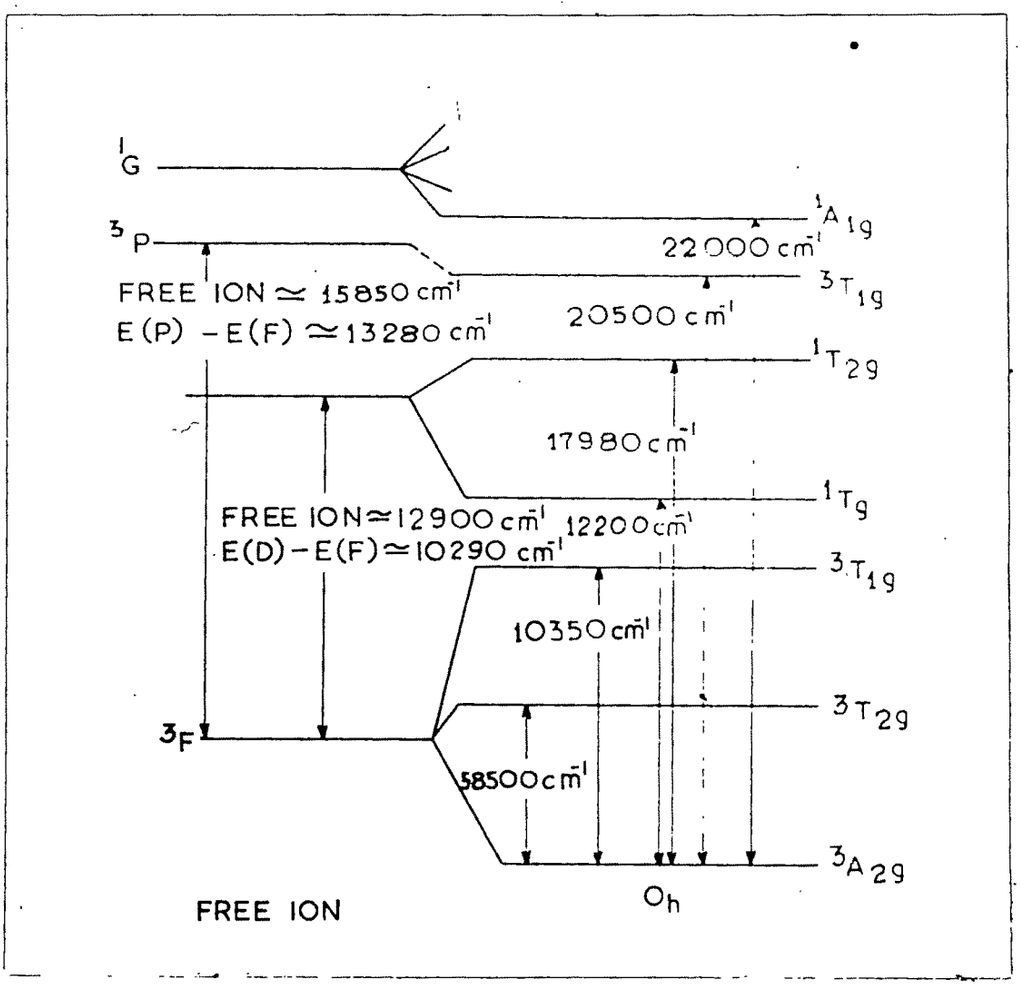

Fig.16. Octahedral energy level scheme of various Stark levels of Ni^{2+} in $CsCdCl_3$. Observed separations are indicated by arrows (Not to scale).

is found to be $\sim$ 585 cm^{-1}. With this value of Dq, the state $^3T_{1g}$ (^3F) should be $\sim$10620 cm^{-1} higher than $^3A_{2g}$. In our room temperature spectrum the moderately wide band at 10250 cm^{-1} has been assigned to $^3A_{2g} \longrightarrow {}^3T_{1g}$ (F) transition. The sharp main band at 20300 cm^{-1} has been identified for the last remaining spin allowed transition $^3A_{2g} \longrightarrow {}^3T_{1g}$ (P). The shoulder of the main band at 18540 cm^{-1} has been assigned to the spin-forbidden transition $^3A_{2g} \longrightarrow {}^1T_{2g}$, a split component of ^1D term. In addition to the above bands, there is also a small hump in the region 12000 cm^{-1} to 12250 cm^{-1} which appears to arise from $^3A_{1g} \longrightarrow {}^1E_g$ (^1D) as will follow from our later discussion. From the above transitions and using the following relations for $3d^8$ ions

$$\begin{aligned} {}^3F &= F_o - 8F_2 - 9F_4 \\ {}^3P &= F_o + 7F_2 - 84F_4 \\ {}^1D &= F_o - 3F_2 + 36F_4 \end{aligned} \qquad (104)$$

where F's are Slater integrals, the evaluated values of $F_2 \sim 1304$ cm^{-1} and $F_4 \sim 84$ cm^{-1} are found to be reduced from their free ion values. With the Dq value of 585 cm^{-1}, the term distances $^3P - {}^3F \sim$ 13280 cm-1 and $^1D - {}^3F \sim 10290$ cm^{-1} are also found to be less than their free ion values (Table 16). Though some of these reductions may be accounted for as the effect of covalency, at least some may be accounted for by configurational interaction[148]. The values of these optical parameters along with their free ion values are given in Table 16. As in the case of Co^{2+} in $CsCdCl_3$, Ni^{2+} has also

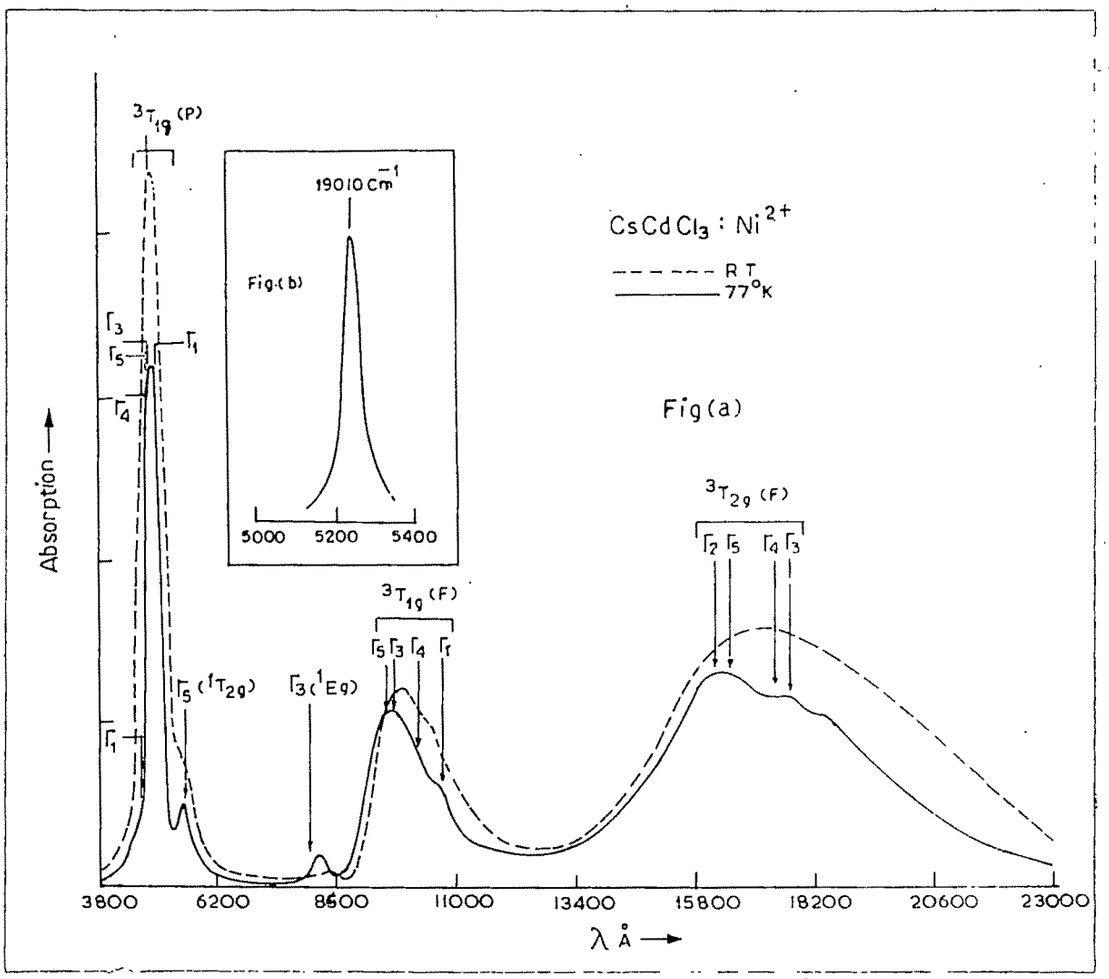

Fig.17(a). Absorption spectrum of Ni^{2+} in $CsCdCl_3$. The dotted line is the room temperature spectrum and the solid line that taken at 77°K. The computed energies with (Dq = 585 cm^{-1} , F_2 = 1302 cm^{-1}, F_4 = 84 cm^{-1} and ζ = -240 cm^{-1}) of the spin-orbit levels are shown by vertical arrows.

Fig.17(b). Shows the band Γ_1 ($^3T_{1g}$) observed in PGS-2 spectrograph in single beam recording arrangement.

a low Dq in comparison with oxide octahedra (860 cm^{-1}) (in (MgO)[35], but it is near to that of the octahedral chloride $KMgCl_3 : Ni^{2+}$ (552 cm^{-1})[115].

At liquid nitrogen temperature almost all the bands (Fig. 17a solid line) shifted towards shorter wave lengths and became narrower with less optical density. The broad band of $^3T_{2g}$ is found to be split into three components at 5452 cm^{-1}, 5714 cm^{-1} and 6136 cm^{-1}, presumably due to spin-orbit splitting, since we could not observe appreciable polarization effects in these components. It would appear that the effect of the small trigonal field is mostly masked by the large spin-orbit coupling in the present case, and hence mixed polarization results. Of the other two spin allowed triplets $^3T_{1g}$ (F) and $^3T_{1g}$ (P) which we have observed at 10250 cm^{-1} and 20300 cm^{-1}, respectively, at room temperature, $^3T_{1g}$ (F) is found to be split up into 10350 cm^{-1} and 9620 cm^{-1} and $^3T_{1g}$ (P) has shifted to 20500 cm^{-1} at liquid nitrogen temperature. The spin-forbidden transition of $^3A_{2g} \rightarrow {}^1T_{2g}$ is now clearly separated from the main transition of $^3T_{1g}$ (P) having peak position at 17980 cm^{-1}. The 12000 cm^{-1} band ($^3A_{1g} \rightarrow {}^1E_g$) ($^1D$)) observed at room temperature, becomes prominent and shifts to 12200 cm^{-1} at low temperature. Besides these, we have observed a sharp band at 19010 cm^{-1}, assignment of which is considered later.

Table 16 : Optical parameters of Ni^{2+} doped in $CsCdCl_3$ and $KMgCl_3$ and their free ion values in relevant units

Ions	Chlorine-metal	E(P)-E(F)	E(D)-E(F)	F_2	F_4	B	C/B	Dq	λ
$CsCdCl_3$: Ni^{2+}	(2.59 Å)	13280	10290	1304	84	884	3.325	585	240
$KMgCl_3$: Ni^{2+} (J. Brynestal et al, 1966)[115]	(2.5 Å)	12795	10915	1328	95	853	3.896	552	275
Free Ion	-	15850	12900	1625	120	1042	3.89	-	-

In order to explain the fine structure of the spectrum at $77^{0}K$ we used Liehr-Ballhausen model[52] of $3d^{8}$ in cubic environment. The four parameters in this model (Dq, F_2, F_4 and λ) are treated as empirical variables. Of these four parameters, Dq, F_2 and F_4 are evaluated earlier from our room temperature spectrum, and the value of the spin-orbit coupling constant λ (λ is equal to one half the Condon and Shortly[40] spin orbit coupling constant ζ_{3d}) was taken from our magnetic measurement. As we are unable to observe any polarization effect and also from magnetic measurement the axial field is found to be small, we did not take into consideration the trigonal field effect in the present context, though this is certainly present, and is important in accounting for the magnetic anisotropy. We used 1130 IBM data processing machine at Computation Centre, Calcutta University, Calcutta, and the roots and energy matrices are given in Table 17. The best fit of our calculated values with those observed transitions is found to be at Dq = 585 cm^{-1}, F_4 = 84 cm^{-1} and λ = -240 cm^{-1}. Calculated energy levels along with observed values are given in Table 18.

Table 17 : The matrix elements of secular equation of Ni^{2+} (d^8) (Liehr, Ballhausen, 1959)[52] with the set of parameter Dq = 585 cm^{-1}, F_2 = 15.5F_4, F_4 = 84 cm^{-1} and λ = 240 cm^{-1}. The eigenvalues are in 2nd coluum from the left.

Term	Eigenvalues cm^{-1}	$^3A_{2g}(t_{2g}^6 e_g^2)$	$^3T_{2g}(t_{2g}^5 e_g^3)$	$^3T_{1g}(t_{2g}^5 e_g^3)$	$^1T_{2g}(t_{2g}^5 e_g^3)$	$^3T_{2g}(t_{2g}^4 e_g^4)$	$^1T_{2g}(t_{2g}^5 e_g^3)$
Γ_5	-18279.6	-18192.0	- 678.8	0.0	-480.0	0.0	0.0
	-12215.9	- 678.8	-12222.0	- 207.8	169.7	415.6	-587.8
	- 7877.5	0.0	- 207.8	-2046.0	293.9	5052.0	-339.4
	- 394.9	- 480.0	169.7	293.9	594.0	587.8	2494.6
	2488.8	0.0	415.6	5052.0	587.8	587.8	-339.4
	8175.2	0.0	- 587.8	- 339.4	2494.6	-339.4	7326.0

Term	Eigenvalues cm^{-1}	$^3T_{2g}(t_{2g}^5 e_g^3)$	$^3T_{1g}(t_{2g}^5 e_g^3)$	$^3T_{1g}(t_{2g}^4 e_g^4)$	$^1T_{2g}(t_{2g}^5 e_g^3)$
Γ_4	-12521.5	-12462.0	- 207.8	- 415.6	- 293.9
	- 8525.7	- 207.8	-1806.0	-5532.0	- 169.7
	2715.0	- 415.6	-5532.0	-4044.0	- 339.4
	4142.2	- 293.3	- 169.7	- 339.4	4122.0

Table 17 (Contd.)

Term	Eigenvalues cm^{-1}	$^1E\ (e_g^2 t_{2g}^6)$	$^3T_{2g}$ $(t_{2g}^5\ e_g^3)$	$^3T_{1g}$ $(t_{2g}^5\ e_g^3)$	$^3T_{1g}$ $(t_{2g}^4 e_g^4)$	^1E_g $(t_{2g}^4 e_g^4)$
Γ_3	-12632.7	-5256.0	- 587.8	- 587.8	0.0	3055.3
	- 7990.6	- 587.8	-12462.0	360.0	720.0	0.0
	- 5765.7	- 587.8	360.0	-2046.0	-5052.0	678.8
	2329.4	0.0	720.0	-5052.0	-3564.0	339.4
	8057.6	3055.3	0.0	678.8	339.4	7326.0

Term	Eigenvalues cm^{-1}	$^1A_{1g}(e_g^2 t_{2g}^6)$	$^3T_{1g}(t_{2g}^5\ e_g^3)$	$^3T_{1g}(t_{2g}^4 e_g^4$	$^1A_{2g}(t_{2g}^4 e_g^4)$
Γ_1	- 8951.8	7680.0	831.3	0.0	11522.4
	1745.3	831.3	-1686.0	-5772.0	678.8
	2884.1	0.0	-5772.0	-4326.0	- 678.8
	30074.3	11522.4	678.8	- 678.8	24084.0

Table 18 : Observed and predicted energies of the spin-orbit states of Ni^{2+} in $CsCdCl_3$ with Dq = 585 cm^{-1}, F_2 = 1302 cm^{-1}, F_4 = 84 cm^{-1} and λ = -240 cm^{-1}

Excited states	Spin-orbit designation	Calculated x 10^{-3} cm^{-1}	Observed (77^0K) x 10^{-3} cm^{-1}
$^3T_{2g}$	Γ_3	5.65	5.45
	Γ_4	5.76	5.71
	Γ_5	6.06	6.02 - 6.21
	Γ_2	6.18	
$^3T_{1g}$	Γ_1	9.33	9.62
	Γ_4	9.75	
	Γ_3	10.30	10.35
	Γ_5	10.40	
^1E_g	Γ_3	12.50	12.20
$^1T_{2g}$	Γ_5	17.88	17.98
$^3T_{1g}$ (P)	Γ_1	20.02	19.01*
	Γ_3	20.61	20.50
	Γ_5	20.77	
	Γ_4	20.99	-
$^1A_{1g}$	Γ_1	21.16	22.00

* This was observed in PGS 2 spectrograph (Fig. 17b) recorded by a photomultiplier (1P-28) in a single beam arrangement.

II. Magnetic Studies

Since this crystal has very small anisotropy (0.7% to 0.9%), great care was taken in grinding the crystal to a symmetric shape to eliminate shape effects. Ionic susceptibilities and anisotropies, obtained from experimental crystalline values using Eqn. (75) and (76) has been plotted in Table 19 at intervals of 20°K. The product $\Delta K.T$ vs. T and $\bar{K}$ vs T are given in Fig. 18.

Table 19 : Magnetic susceptibility and anisotropy of $CsCd_{1-x}Ni_xCl_3$, where x = 3.1 mol % (graphically interpolated values)

Temperature °K	$\Delta\chi \times 10^6$	$(K_{\parallel} - K_{\perp}) \times 10^6$	$\chi_{\perp} \times 10^6$	$\bar{K} \times 10^6$
300	18.4	27.7	4181	4187
280	19.9	29.9	4447	4454
260	21.6	32.5	4761	4768
240	23.8	35.7	5125	5133
220	26.4	39.7	5551	5560
200	29.8	44.8	6066	6076
180	34.5	51.8	6695	6707
160	39.6	59.5	7483	7496
140	47.2	70.8	8488	8504
120	58.0	87.0	9824	9844
100	73.2	109.8	11696	11720
80	98.4	147.7	14467	14500

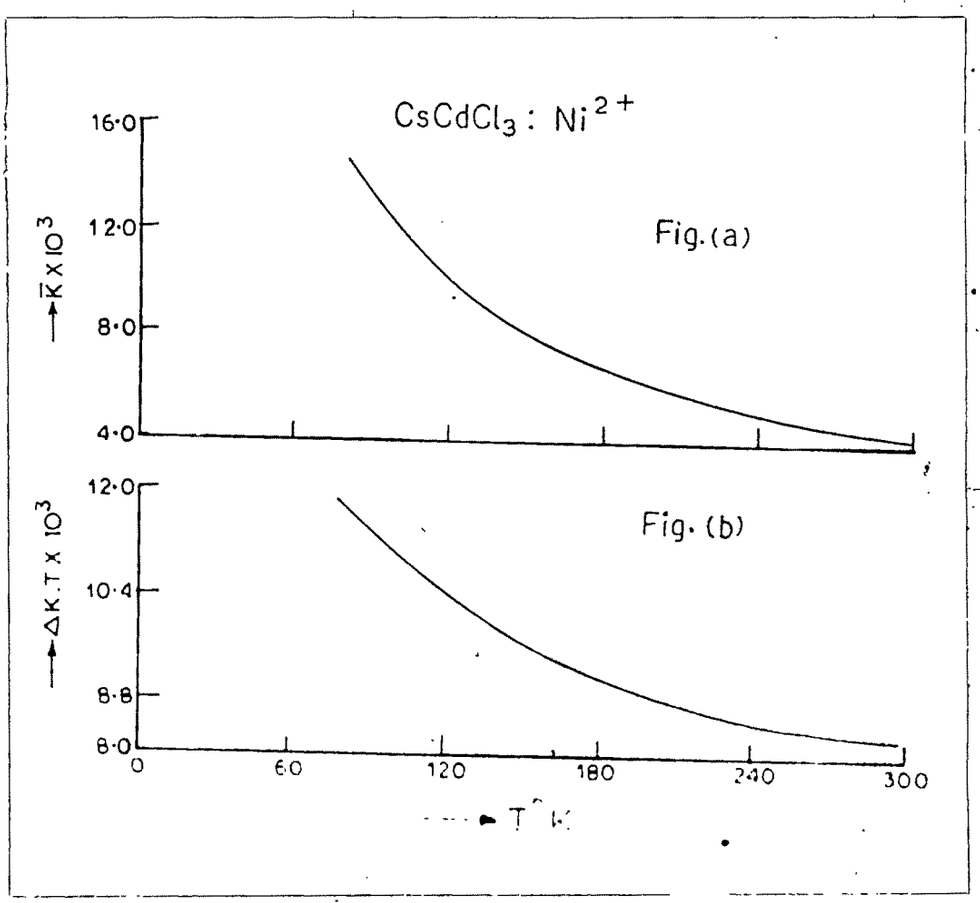

Fig.18(a). Variation of the susceptibility (K) temperature ($CsCdCl_3$: Ni^{2+})

Fig.18(b). Variation of the product of anisotropy and temperature (K.T) with temperature ($CsCdCl_3$: Ni^{2+})

A. Fine Structure Energy Levels and Magnetic Susceptibility of Trigonally Distorted Octahedral Ni^{2+} [149]

Energies of the trigonal doublet and singlet which are the split components of the excited orbital triplets of ^3F term and of the ground orbitally non-degenerate state are given by

$$E_{0,4} = \tfrac{1}{2}\left[(-6Dq + \tfrac{3}{10}A_2 + \tfrac{27}{2}A_4 \mp \left\{(18Dq + \tfrac{3}{10}A_2 - \tfrac{1}{2}A_4)^2 + \tfrac{4}{5}(3A_2 - 5A_4)^{1/2}\right\}^{1/2}\right]$$

$$E_{1,3} = \tfrac{1}{2}\left[(4Dq - \tfrac{9}{10}A_2 - 9A_4) \mp \left\{(8Dq + \tfrac{3}{5}A_2 - 8A_4)^2 + \tfrac{1}{20}(3A_2 - 40A_4)^2\right\}^{1/2}\right]$$

$$E_2 = -2Dq + 3/2\ A_2 + 9/2\ A_4 \qquad (105)$$

where the first and the second subscripts on E refer to the -ve or +ve sign appearing within the square brackets in Eqn. (105), and A_2 and A_4 and Dq are the ligand field parameters.

Writing the spin Hamiltonian of non-degenerate ground state (Eqn. 55) for trigonally distorted $CsCdCl_3 : Ni^{2+}$ for H $\|^{l}$ to Z, the axis of the trigonal symmetry, we have

$$\mathcal{H}_S = D\left[S_z^2 - \tfrac{1}{3}S(S+1) + g_{\|}\beta H_z S_z - \alpha_{\|}\beta^2 K_{\|}^2 H_z^2\right] \qquad (106)$$

and for H $\perp^{r}$ Z

$$\mathcal{H}_S = D\left[S_z^2 - \tfrac{1}{3}S(S+1) - g_{\perp}\beta H_x S_x - \alpha_{\perp}\beta^2 K_{\perp}^2 H_x^2\right] \qquad (106)$$

where

$$D = -(\alpha_{\parallel}\lambda_{\parallel}^{2} - \alpha_{\perp}\lambda_{\perp}^{2})$$

$$g_{\parallel} = 2(1 - \alpha_{\parallel}K_{\parallel}\lambda_{\parallel})$$

$$g_{\perp} = 2(1 - \alpha_{\perp}K_{\perp}\lambda_{\perp})$$

where

$$\alpha_{\perp} = \frac{2(\sqrt{2}a_0a_1 - \frac{1}{2}\sqrt{5/2}\,b_0a_1 + (3/2\sqrt{2})b_0b_1)^2}{E_1 - E_0} + \frac{2(\sqrt{2}a_0b_1 - (1/2)\sqrt{5/2}\,b_0b_1 - (3/2\sqrt{2}\,b_0b_1)^2}{E_3 - E_0}$$

$$\alpha_{\parallel} = (2a_0 + \sqrt{5}\,b_0)/(E_2 - E_0) \qquad (107)$$

the wavefunction coefficients a's and b's are given by

$$a_0 = \{((3/\sqrt{5})A_2 - \sqrt{5}A_4)/(E_0 + 12Dq - 7A_4)\}b_0\,; \quad a_0^2 + b_0^2 = 1$$

$$a_1 = \{((3/4\sqrt{5})A_2 - (2\sqrt{5})A_4)/(E_1 + 2Dq + (3/4)A_2 + (1/2)A_4\}b_1\,; \quad a_1^2 + b_1^2 = 1 \qquad (108)$$

The effect of overlap of ligand charge clouds with central metal charge clouds has been incorporated in the spin Hamiltonian through the introduction of orbital reduction factor $K_{\parallel}$ and $K_{\perp}$ and the anisotropic reduced spin-orbit coupling coefficient $\lambda_{\parallel}$ and $\lambda_{\perp}$.

Operating with the spin Hamiltoniam H_s Eqn. (106) on the spin state $|1\rangle$, $|0\rangle$ and $|-1\rangle$, we have the energies

(a) $H \parallel^{l} Z$

$$E_1 = (1/3)D + g_{\parallel}\beta H_z - \alpha_{\parallel} K_{\parallel}^2 H_z^2$$

$$E_0 = -(2/3)D - \alpha_{\parallel} K_{\parallel}^2 \beta^2 H_z^2$$

$$E_{-1} = (1/3)D - g_{\parallel}\beta H_z - \alpha_{\parallel} K_{\parallel}^2 \beta^2 H_z^2$$

(b) $H \perp^{T} Z$

$$E_1 = \tfrac{1}{2}\left[-(1/3)D - 2\alpha_{\perp} K_{\perp}^2 \beta^2 H_x^2 + \sqrt{D^2 + 4g_{\perp}^2 \beta^2 H_x^2}\right.$$

$$E_0 = (1/3)D - \alpha_{\perp} K_{\perp}^2 \beta^2 H_x^2$$

$$E_{-1} = (1/2)\left[-(1/3)D - 2\alpha_{\perp} K_{\perp}^2 \beta^2 H_x^2 - \sqrt{D^2 + 4g_{\perp}^2 \beta^2 H_x^2}\right. \qquad (109)$$

The expression of magnetic susceptibilities (c.f. Eqn. 57) can be written as

$$K_{\parallel} = (N\beta^2/k)\left\{2k\alpha_{\parallel} K_{\parallel}^2 + (2g_{\parallel}^2/3T) - (3Dg_{\parallel}^2/9kT^2)\right\}$$

$$K_{\perp} = (N\beta^2/k)\left\{2k\alpha_{\perp} K_{\perp}^2 + (2g_{\perp}^2/3T) + (Dg_{\perp}^2/9kT^2)\right\} \qquad (110)$$

or

$$\bar{K} = (N\beta^2/k)\left[(2/3)k(\alpha_{\parallel} K_{\parallel}^2 + 2\alpha_{\perp} K_{\perp}^2) + (2\bar{g}^2/3T)\right. \qquad (111)$$
$$\left. - (2D/9kT^2)(g_{\parallel}^2 - g_{\perp}^2)\right]$$

and $$\Delta K = (N\beta^2/k)\left[2k(\alpha_{\parallel} K_{\parallel}^2 - \alpha_{\perp} K_{\perp}^2) + (2/3T)(g_{\parallel}^2 - g_{\perp}^2)\right. \qquad (112)$$
$$\left. - (D/9kT^2)(2g_{\parallel}^2 + g_{\perp}^2)\right]$$

$g_{\parallel}^2 - g_{\perp}^2$ was found to be small compared to $\bar{g}^2 = 1/3[g_{\parallel}^2 + 2g_{\perp}^2]$

B. Parametric Fittings and Discussion

In correlating our experimental values with the above theory we have found by trial and error a set of value of , λ'/Λ and k'/Λ which fit best with our observations. Calculated and observed values are given in Table 20. We are able to explain our optical observation with spin-orbit coupling as $-240\ cm^{-1}$ and this is in good agreement with magnetic $\lambda_{\parallel} = -238.5$ and $\lambda_{\perp} = -235$. Our parametric values of zero field splitting, $D = -1.95\ cm^{-1}$ and $g_{\parallel} = 2.198$ and $g_{\perp} = 2.195$ at $300^{0}K$ is very near to e.s.r. findings of $CsMgCl_3 : Ni^{2+}$ at $300^{0}K$, $D = -1.92$ and $g = 2.27$ by McPherson[150]. Though in case of Fe^{2+} and Co^{2+} we could fit our experimental results with same set of parameters, we were not able to fit our results in the present case for the whole range of temperature with a fixed set of parameters; though the agreement between calculated and observed $\bar{K}$ is very good, there is large difference in ΔK. In the previous cases the discrepancy, which is very small but systematic may be due to small changes in the crystal field with temperature; which, however, could not make much difference in the large anisotropy involved in those cases. In our present case, where the total anisotropy is small, it is much more affected due to even small changes in α'/Λ i.e. parameters connected with trigonal field. So keeping k'/Λ and λ'/Λ fixed we have changed α'/Λ and so also the related parameters by very small amount at different temperatures to fit our experimental data.

Table 20 : Calculated ligand field parameters for $CsCdCl_3 : Ni^{2+}$ *

$Dq = 585\ cm^{-1}$

$\lambda_{\parallel} = -238.5$ $\qquad$ $\lambda_{\perp} = -235\ cm^{-1}$

$K_{\parallel} = 0.74$ $\qquad$ $K_{\perp} = 0.761$

Temp. ^{o}K	$\alpha_i \times 10^4$	g_i	$-D\ cm^{-1}$	$\Delta K \times 10^6$	$\bar{K} \times 10^6$
300	$\alpha_{\parallel} = 5.621$ $\alpha_{\perp} = 5.452$	$g_{\parallel} = 2.1984$ $g_{\perp} = 2.1950$	1.95	27.7 (27.7)	4146.5 (4187)
200	$\alpha_{\parallel} = 5.51$ $\alpha_{\perp} = 5.37$	$g_{\parallel} = 2.1945$ $g_{\perp} = 2.1920$	1.685	45.43 (44.8)	6171 (6076)
140	$\alpha_{\parallel} = 5.241$ $\alpha_{\perp} = 5.131$	$g_{\parallel} = 2.1850$ $g_{\perp} = 2.1835$	1.47	70.78 (70.80)	8671 (8504)
80	$\alpha_{\parallel} = 4.72$ $\alpha_{\perp} = 4.65$	$g_{\parallel} = 2.1660$ $g_{\perp} = 2.1660$	1.17	148.6 (147.7)	14820 (14500)

* Figures within parenthesis are experimental values.